Microvascularity, blood flow and tissue structure at the subchondral plate using an x-ray fluorescence technique

P. Muthuvelu [a], R.E. Ellis [a], E.M. Green [a], D. Attenburrow [a],

R. Barrett [b], K. Arkill [a], D.B. Colridge[a], C. P. Winlove [a], D. A. Bradley [a] *

[a] Biomedical Physics Group, School of Physics, University of Exeter, Exeter, UK

[b] ESRF, BP 220, F-38043 Grenoble Cedex, France

**Corresponding author; e-mail:d.a.bradley@exeter.ac.uk*

Abstract

The measurement of blood flow and blood in bone and cartilaginous tissues is crucial to understanding of the development of various diseases, but it presents a formidable technical challenge. We have therefore developed a method based on the detection of metallised microspheres using x-ray fluorescence. This approach provides unrivalled sensitivity and spatial resolution and also allows simultaneous measurement of other markers of the metabolic status of the tissue.

Introduction

Articular cartilage is avascular, the conventional opinion being that it receives its nutrition from synovial fluid via the articular surface. Although the subchondral bone possesses a rich blood supply in the mature animal, it is believed to be separated from the cartilage by an impermeable calcified layer [1]. However, quantitative data on blood volume and flow in the subchondral region are extremely scarce, due for the most part to difficulties in studying bone using standard techniques of flow measurement such as radio- or fluorescent-labelled microspheres [2-4] or laser Doppler flowmetry and even in processing for histology. We have therefore sought to develop a modification of the familiar microsphere method, using a synchrotron-based x-ray fluorescence technique which overcomes these difficulties. The approach also allows simultaneous analysis of the elemental composition of the surrounding tissue structure, for instance Ca and Sr whose distribution is of great interest in the context of bone turnover and remodelling, and use of the structure determination methods of μSAXS and μWAXS (micro small- and wide-angle x-ray scattering respectively) for collagen fibre and calcium crystal analysis. Our approach therefore allows local blood flow to be related to tissue architecture and composition. The present report focuses upon investigation of blood flow within subchondral bone of

the equine metacarpophalangeal joint, obtained by trapping of uniformly sized microspheres in the microvasculature, and of the distribution of blood vessels in subchondral bone through detection of Fe bound in haemoglobin. The study is accompanied by determination of Sr and Ca distribution, both in normal tissue and in a focal lesion, the latter being a precursor to osteoarthritis. Interest in Sr distribution arises physiologically from the dynamics of the incorporation of dietary strontium in mineral and recent clinical use of Sr in the treatment of osteoporosis[5].

Experimental

Use has been made of an *ex vivo* perfused equine fore-limbs preparation, fore-limbs being obtained from an abattoir immediately after sacrifice. At the abattoir, in preparation for measurements of flow, a catheter was inserted into the outer medial artery of the forelimb and carefully secured. One to two litres of saline solution were then injected into the medial artery via the catheter, the limb being gently articulated to ensure thorough flushing. The saline solution was injected continuously until there was an absence of blood in the outflow liquid. The leg, with the catheter still in position, was then wrapped in a plastic bag, placed in a cooler box and transported to the laboratory.

Measurements were made on three animals, with no clinical symptoms of gross joint disease. However, on examination a number of early focal lesions were present is some of the limbs. For flow measurements, silver-coated 15 μm diameter microspheres (BioPhysics Assay Laboratory, Inc, Worcester, MA) were introduced into the inflow stream over a known time period. The Ag-coating of each sphere has been estimated to represent ~ 13% of the total weight of a microsphere. Immediately after flow was stopped, the limb was fixed in formal saline. Limbs for blood volume measurement were fixed intact immediately after amputation. In either case, sections ~ 1 mm thick (established in preliminary experiments to be the optimum compromise between attenuation, spatial resolution and tissue damage) were cut perpendicular to the articular surface.

In preliminary experiments aimed at measuring blood content through detection of K_α fluorescence from haemoglobin iron (Fe K_α 6.40 keV) the cut sections, mounted in a humidified chamber, were placed on the sample stage of a Cu tube crystallographic x-ray source at an angle of approximately 45º to the incident beam and also to a hyper-pure Ge detector. From these screening measurements, more sensitive and spatially detailed measurements were made at the ESRF beamline ID18F, using a similar geometry. At the latter facility, and with the aid of a scanning stage, individual energy dispersive x-ray

fluorescence measurements were made, using typically a beam spot size of 50 μm and acquisition time of 10 s per point to obtain an array of measurements over a total area of up to 6 mm x 6 mm. Image analysis was performed using Image J (NIH) [6]. Details of the source condition and detectors used at the ID18F beamline are available from the ESRF website (www.esrf.fr). Using an excitation energy of 27 keV, the silver K_α fluorescence was detected at 22 keV. To investigate the organisation of collagen and mineral both small angle x-ray scattering and wide-angle x-ray scattering measurements have also been performed on the same tissue. These latter data will be reported elsewhere.

Results and Discussion

A Ca K_α fluorescence mapping for a normal region of tissue taken from the metacarpal condyle (sagittal ridge) is shown in Fig. 1, providing an indication of bone mineral density over the field of view. Figs. 2 and 3 provide corresponding mappings of the distribution of the Sr and Ag K_α fluorescence respectively from the same bone section. While broad correlation is to be observed between the distribution of Ca and Sr intensities, at the more detailed level there are significant differences, particularly in regard to their relative presence within the outer shell of the subchondral plate and in the individual trabecula.

For detection of silver, the μXRF technique was found sufficiently sensitive to allow detection down to single microspheres; the variation of intensity of Ag K_α fluorescence seen in Fig. 3 is due in part to differential attenuation of the XRF signal from microspheres located throughout the depth of the ~1mm thick bone section. The extent to which the variations in intensity may represent multiple particles in a single vessel or juxtaposed capillaries remains to be established. The spatial resolution evident in the figure has not been obtained in previous microsphere studies and raises questions about the mechanisms of microsphere trapping that have not been addressed. The absence of flow above the calcified layer is immediately apparent and the distribution of fluorescence correlates well with the capillary density observed in histological sections (Fig. 4a) and our own Fe data (see below). In bone sections from all three animals, capillaries of diameter 15 μm were detected as close as 1.5mm below the calcified layer[7].

In a follow-up study measuring capillary blood volume, Fe K_α fluorescence (Fig 4b) has been detected as close as ~ 0.7 mm from the tidemark (the latter providing an indication of where the calcified layer begins). The sensitivity of the measurement is due to the high concentration of iron in haemoglobin.

For the future, it is intended that raster scans will be performed over a relatively fine mesh of measurement points, to determine the extent to which the blood supply approaches the tidemark.

Finally, Fig 5 shows a mapping of Ca K_α fluorescence in the vicinity of a focal lesion, the cartilaginous region being just visible. Using this data and a simultaneous mapping of Sr K_α fluorescence, distributions of Ca and Sr have been obtained. Figs 5b and 5c show examples. The ratio of the respective K_α fluorescence intensities normalises for sample dependent effects (neglecting self-absorption) and allows the distribution of the two elements to be measured with unrivalled sensitivity and spatial resolution. The use of such information in study of the metabolic status of the tissue is on-going.

Conclusions

Investigations have been made on the microvasculature and composition of subchondral bone of the third equine metacarpophalangeal joint. For sections of the bone ~1mm thick, use has been made of a synchrotron x-ray fluorescence system to locate entrapped silver-doped 15μm microspheres and the natural presence of Ca and Sr . Microcirculatory blood was detected using Fe fluorescence from haemoglobin. The measurements of blood flow and volume, combined with elemental mappings and microdiffraction analysis of tissue structure, provide a new approach to the analysis of relationships between blood flow and tissue pathophysiology.

References

1. R.A. Stockwell, Biology of Cartilage Cells, Cambridge Univ. Press. 1979.

2. F.W. Prinzen, J.B. Bassingthwaighte, Cardiovasc. Res. 45 (2000) 13.

3. Y. Nakajima Y, N. Akizuki, Y. Kimuar, H. Kohguchi, A. Tanaka, M. Chujo, N. Hattan, Y. Shinozaki, A. Iida, S. Handa, H. Nakazawa, H. Mori, Am. J. Physiol: Heart Circ. Physiol. 277 (1999) H2353.

4. F.W. Prinzen, R.W. Glenny, Cardiovas Res. 353 (1994) 337.

5. S.G. Dahl, P. Allain, P.J. Marie, Y. Mauras, G. Boivin, P. Amman, Y. Tsouderos, P.D. Delmas, C. Christiansen, 28 (2001) 446.

6. ImageJ is a public domain Java image processing program developed at the National Institute of Health, Bethesda, MD, USA.

7. P. Muthuvelu, R.E. Ellis, E.M. Green, B. Sheldon, D. Attenburrow, R. Barrett, M. Drakopoulos, C.P. Winlove, D.A. Bradley, Rad. Phys. Chem. 71 (2004) 961.

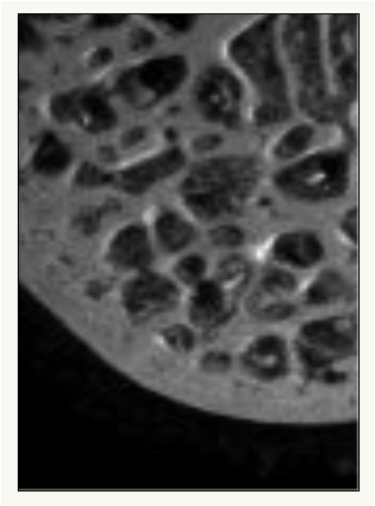

Fig.1 Raster scan, showing detection of Ca K_α fluorescence, from a bone section ~ 1mm thick. The field of view is 4 mm wide by 6 mm long.

Fig.2 Raster scan of the same bone section and field of view as in Fig. 1, detecting K_α fluorescence from Sr in bone. The image, less distinct than that of Ca K_α fluorescence, is partly a result of non-structural Sr.

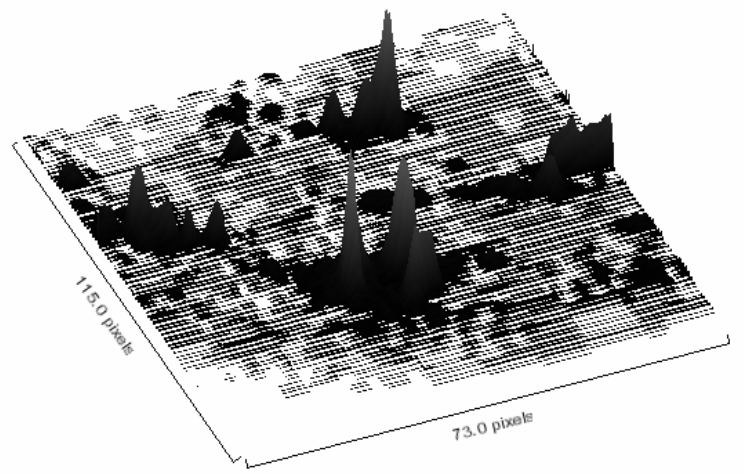

Fig.3a. Surface plot of the lower left hand corner of the cartilage-bone section depicted in Figs 1 and 2, detecting Ag K_α fluorescence from 15 μm Ag-coated spheres lodged at 1.5 mm and deeper within the subchondral bone surface, each side of pixel representing 0.05 mm. The Ag K_α fluorescence peaks indicate rich supply of blood within the subchondral bone.

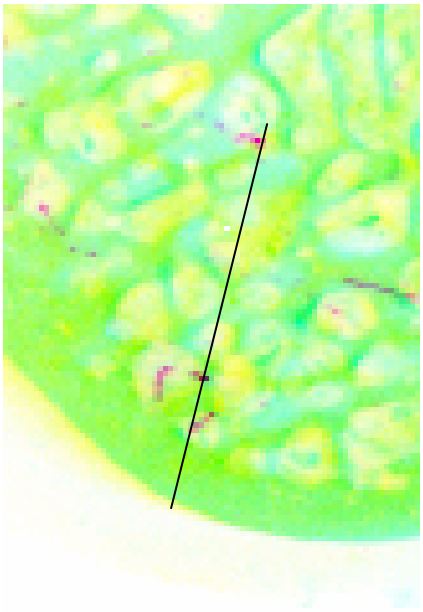

Fig 3b False colour overlay of the bone section and identical field of view depicted in Figs. 1 and 2, together with the Ag K_α fluorescence raster scan from which Fig. 3a was produced. Visible are a number of the silver-coated microspheres. The distribution of calcium and strontium are represented by the darker and lighter shading respectively.

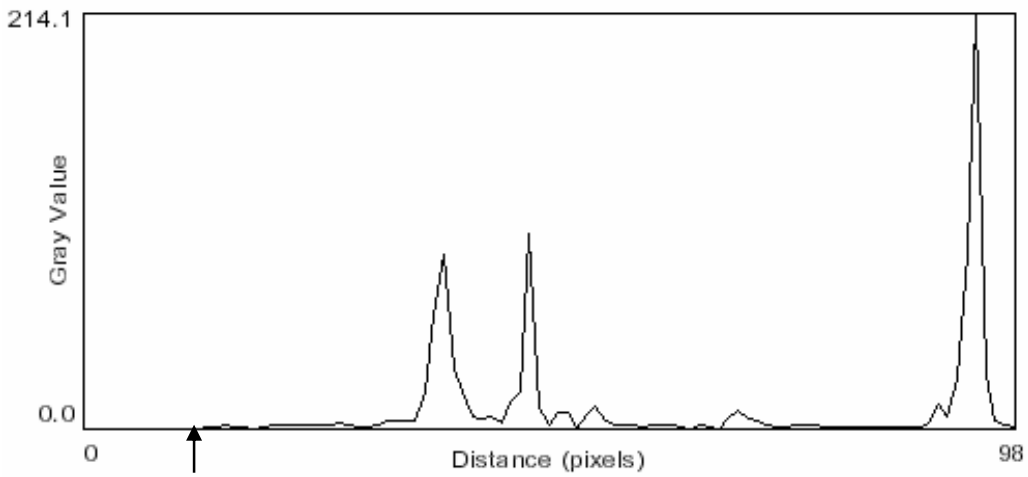

Fig. 3c. Intensity profile of K_α fluorescence due to the three Ag-coated microspheres located along the line indicated in Fig 3b. As before, each pixel represents 0.05 mm. An arrow indicates the position of the articular surface.

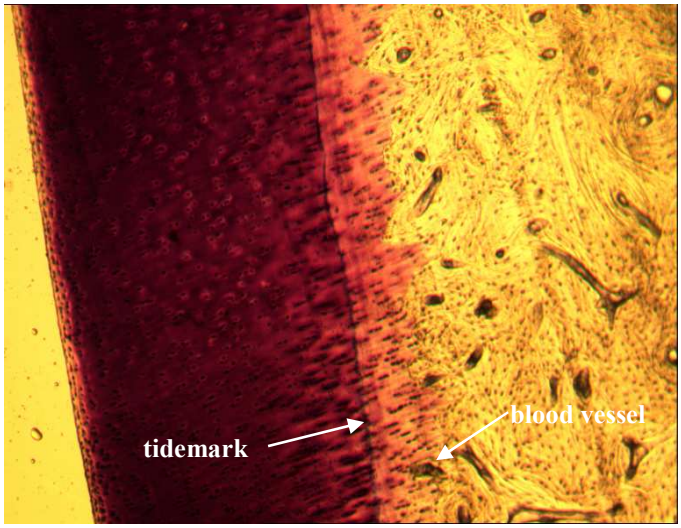

Fig. 4a. Typical histological section of articular cartilage, taken in this example from a 14 yr old animal; the 20 μm thick section has been stained with 0.13% toluidine blue for 4 min. For the particular field of view the minimum distance from the tidemark (indicated by an arrow) to the nearest blood vessel is 125 μm.

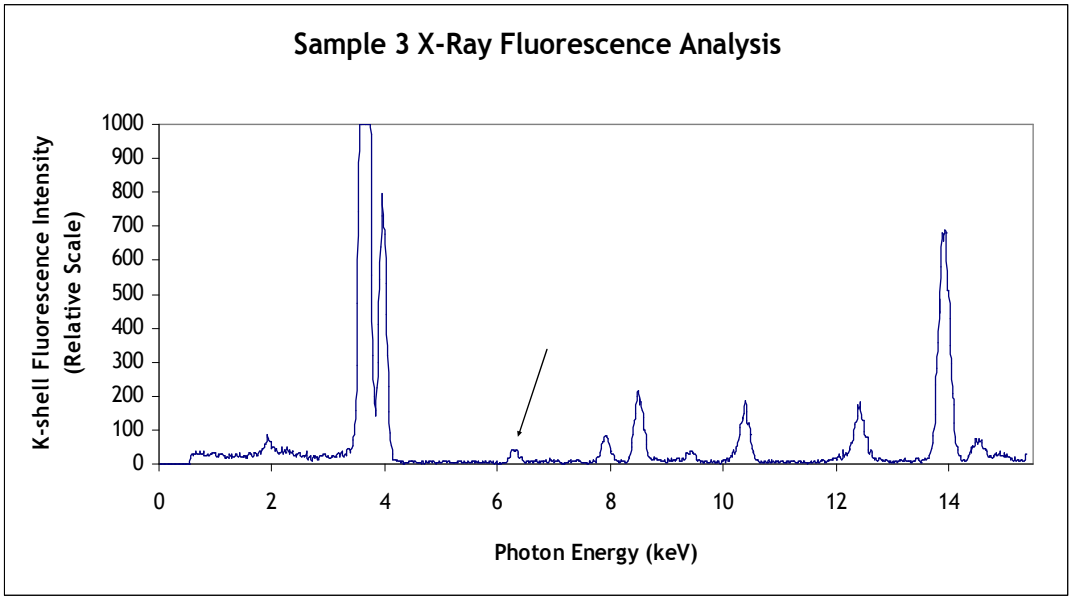

Fig. 4b. Intensity profile of Fe K_α fluorescence located along a line approximately perpendicular to the articular surface of normal bone, beginning at the tide mark. Blood supply is evident as close as ~ 1.4 mm from the cartilage surface.

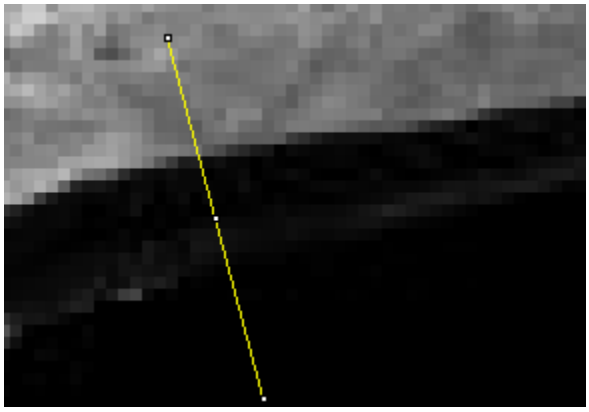

Fig. 5a. Variations of Ca K_α fluorescence intensity in the vicinity of a focal lesion. The cartilaginous region is just visible. Measurements of Ca- and Sr K_α fluorescence intensity through the lesion have been taken from the respective fluorescence maps, along the line indicated.

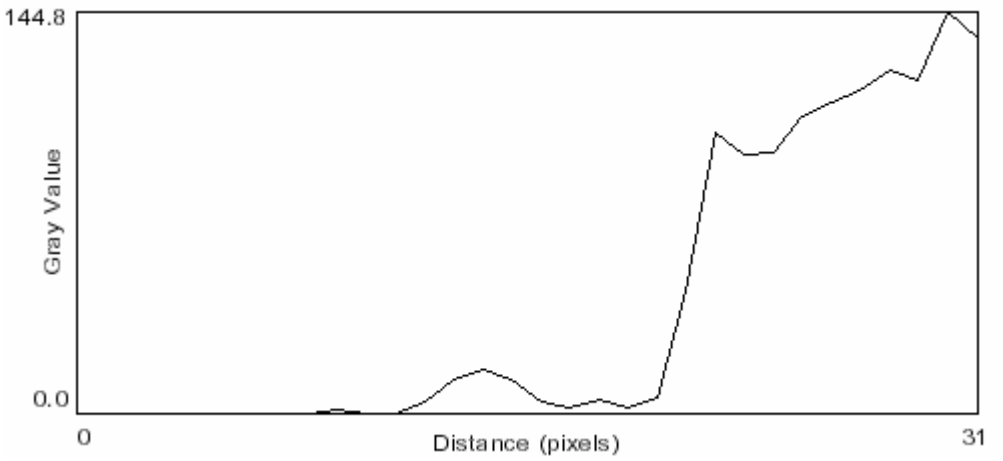

Fig. 5b. Ca K_α fluorescence intensity variation in the vicinity of the focal lesion depicted above, along the indicated line. The scan begins at some point outside of the cartilage surface (1 pixel having a side equivalent to 0.05 mm).

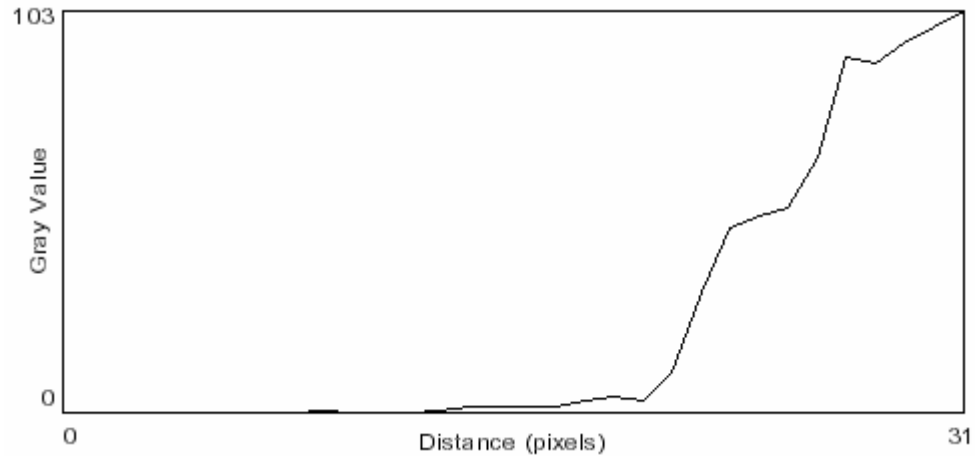

Fig. 5c. Sr K_α fluorescence intensity scan along the same line as in Fig 5b, measured in the counterpart Sr K_α fluorescence intensity map.